

Image Segmentation and Tracking Under Max/Min Flow Framework

Authors
Affiliation

Abstract

In this paper, the boundary leaking is firstly analyzed on the geodesic active contour model in detail. Then the Max/Min flow framework is generalized and applied to deal with boundary leaking on image segmentation and region tracking applications. It is proved that the generalized Max/Min flow framework could reach a steady state solution. Experiments show that this generalized framework is a flexible computational framework, and many methods and strategies can be combined into this framework simply.

Keywords: *Max/Min flow framework, boundary leaking, Image segmentation, Region tracking*

1. Introduction

Methods of curve evolution for segmentation, tracking and registration were firstly introduced in computer vision by Kass, et al. in [1]. These evolutions were reformulated as the geodesic active contour model under the Euclidean curve shorting flow framework by Caselles, et al. in the context of PDE-driven curves and surfaces [2]. Level set methods were firstly introduced by Osher and Sethian in the context of fluid mechanics in [3]. They provided both a nice theoretical framework and efficient practical computational tools for solving such PDE's. There has been a lot of literature that addresses its mathematical foundation and various applications. But then, there are some challengeable problems in implementation of level set methods, such as distance function [4], boundary leaking [5], etc. In this paper, we are concerned about the boundary leaking problem, which resulted from the original geodesic active contour model. In order to deal with it, many constraint terms have been introduced in these PDE's, such as weighted area gradient flow [5], gradient vector flow [6], edge-flow [7], etc. It is possible to suppress the boundary leaking if the evolving tendency of flow can be controlled. This is easy to be implemented under the Max/Min flow framework.

The Max/Min flow scheme was firstly proposed in [8,9] for image enhancement and denoising. However, it is a flexible computational framework, and many methods and strategies can be combined into this framework. These sophisticated methods are usually used to determine the evolving tendency of flow. Thus, in this paper, we

generalized this scheme, and proved that this general computational scheme could reach a steady state solution. Furthermore, it was applied to the image segmentation and region tracking applications for suppressing the boundary leaking. In addition, under this general framework, it can be noticed that the forms of speed function for the image segmentation and region tracking are similar, while their different decision rules (boundary conditions) can be defined respectively. This simplifies the design of speed function for various different problems. Since this framework is an open general framework, it is easy to change decision rules for other different problems.

Recently the problem of partial volume estimation has attracted a wide interest for image segmentation. In essential, it is to identify different materials within a small region of image, only its datasets is volume data. In [10], the partial volume modeling was proposed, which could classify for each voxel by modeling the voxel histograms. In [11], the grey-level distributions were modeled as a linear combination of Gaussian distributions for the pure material and the Gaussian-triangle convolution for each possible mixture. The distributions of the grey-level slope were modeled as a linear combination of Rayleigh distribution for pure material and Rician distribution for each possible mixture. These statistic models were used to approximate the real model. In [12], the region competition algorithm was presented, which dealt with the mixture model by using a neighbor window of each pixel. In our approach, these sophisticated statistic models or algorithms would be combined with the curve evolution model under this general Max/Min flow framework, so as to ensure the evolving tendency of flow rightness.

Another example of the deformable model is to use level set methods in solving the region tracking problem [13-15]. Because the goal of these tracking algorithms is to extract the boundaries of moving objects, some methods and strategies in the implementation of level set methods for image segmentation are used in the implementations of these region tracking algorithms. Thus, there are some similar problems between these two applications. In the following applications, it can be noticed that their forms of level set equations are similar, while their different boundary conditions can be defined respectively under the Max/Min flow framework.

This paper is organized as follows. In section 2, the boundary leaking is firstly analyzed in detail on the

geodesic active contour model. Then, the Max/Min flow framework is briefly introduced and generalized in section 3. In section 4, the generalized Max/Min flow framework is applied to deal with the boundary leaking on the image segmentation and region tracking applications. Finally, our conclusions appear in section 5.

2. Boundary Leaking

The boundary leaking was firstly observed on CT medical image segmentation in [5]. In fact, it is an intrinsic fault of the original geodesic active contour model. This deformable model is usually written as,

$$C_t = g(I)\kappa_c \mathbf{N}_c - (\nabla g \cdot \mathbf{N}_c) \mathbf{N}_c,$$

where, κ_c is the Euclidean curvature of evolving curve $C(t)$, \mathbf{N}_c is the unit inward normal of $C(t)$, $g(I)$ is usually defined as a monotonically decreasing function of the intensity gradient $|\nabla I|$, which attracts the evolving curve towards the object boundary. Using the level set framework, we can obtain its level set representation as follow,

$$\phi_t = g(I)\kappa_c |\nabla \phi| + \nabla g \cdot \nabla \phi, \quad (1)$$

with the initial condition $\phi(0, C) = \phi_0(C)$, and its speed function $F = g(I)\kappa_c - \nabla g \cdot \mathbf{N}_c$. It is easy to see that the curvature term in the speed function is the known Euclidean heat flow, which is used for curve smoothing and evolution. This is the basic form of Euclidean heat flow. In practice, if only the dynamic balance is reached between the curvature term and the second term, the evolving curve can obtain a trivial steady state.

Furthermore, expanding the speed function, we yield

$$F = g(I)\kappa_c - g'D^2I \left\langle \frac{\nabla I}{|\nabla I|}, \mathbf{N}_c \right\rangle,$$

where D^2I denotes the Hessian of the intensity I . Assume that the evolving curve has converged at the real boundary. Then the unit vector of intensity gradient and the normal of $C(t)$ should be identical, i.e. $-\mathbf{N}_c = \nabla I / |\nabla I|$. Obviously, the second term should be the second derivate of I in direction of intensity gradient up to a derivative scale $g'(I)$, and be equal to zero, i.e. $D^2I \left\langle \nabla I / |\nabla I|, \mathbf{N}_c \right\rangle = I_{\eta\eta} = 0$. Because the function $g(I) = \text{minimum} \neq 0$, it is difficult to reach a dynamic balance state at the real boundary. Thus, this scheme is prone to boundary leaking.

Most deformable models are proposed for boundary detection. As the image segmentation, these models can be used to extract the contours of moving object in region tracking, but the input frames are usually enhanced in advance. Region tracking is usually based on the observed inter-frame intensity difference model,

$d(x, y) = I(x, y, t) - I(x, y, t-1)$, where $I(x, y, t)$, $I(x, y, t-1)$ are the current and the previous frame intensity function. And the probability density function of $d(x, y)$ is modeled as a mixture of two Gaussian (or Laplacians) distributions, which are both zero-mean and correspond to the background area and the moving objects area respectively.

In [13,14], the detecting and tracking moving objects in image sequences were formulated in a variational framework. The motion detection only estimates the moving area between the two successive frames. It does not detect the original input frame sequences directly, but detects a new generated frame, which is described as,

$$I_D(X) =$$

$$\max_{Y \in \Omega(X)} \left\{ \frac{pd|_{bg}(d(X)) \cdot pd|_{obj}(d(Y)) + pd|_{obj}(d(X)) \cdot pd|_{bg}(d(Y))}{pd|_{bg}(d(X)) \cdot pd|_{bg}(d(Y)) + pd|_{obj}(d(X)) \cdot pd|_{obj}(d(Y))} \right\},$$

where, $\Omega(X)$ denoted the neighborhood of pixel $X \in R^2$, and $pd|_{bg}(\cdot)$, $pd|_{obj}(\cdot)$ are the probability density function of

the observed inter-frame difference $d(X)$ under the background area (or object area) hypothesis. In this new frame, the moving area has been enhanced. The edge detection operation is applied to this new generated frame in the motion detection part. The next step is the tracking part. Unlike the motion detection, the tracking part detects the boundary of moving object on the original input frames directly.

The detection and tracking problem were described in [13] as an energy minimum problem. The Euclidean curve evolution equation is described as,

$$C_t = \gamma(g(I_D)\kappa_c - \nabla g(I_D) \cdot \mathbf{N}_c) \mathbf{N}_c + (1-\gamma)(g(|\nabla I|)\kappa_c - \nabla g(|\nabla I|) \cdot \mathbf{N}_c) \mathbf{N}_c, \quad \gamma \in [0,1]$$

And its level set representation could be written as,

$$\phi_t = \gamma \left(g(I_D)\kappa_c + \nabla g(I_D) \cdot \frac{\nabla \phi}{|\nabla \phi|} \right) |\nabla \phi| + (1-\gamma) \left(g(|\nabla I|)\kappa_c + \nabla g(|\nabla I|) \cdot \frac{\nabla \phi}{|\nabla \phi|} \right) |\nabla \phi| \quad (2)$$

It is clear that both the motion detection and tracking part adopt the geodesic active contour model, whose speed functions have the common form as in Eq.(1). Thus, the boundary leaking problem exists in the scheme of Eq.(2) too.

If the wrong evolving tendency of flow can be corrected, it is possible to suppress boundary leaking. In our approaches, the schemes of Eq.(1) and Eq.(2) are redefined under the generalized Max/Min flow framework. It can be noticed that the evolving tendency is corrected by the decision rules. This is a main reason why the generalized Max/Min flow framework is introduced.

3. Generalized Max/Min Flow Framework

In [8,9], the Max/Min flow scheme was firstly presented for noise removal and image enhancement. An image is interpreted as a collection of iso-intensity contours, which can be evolved, and speed function is only defined as image intensity curvature, so that sharp boundaries are preserved. Compared to existing techniques, this approach has several distinct advantages. One is to remove noise without too much blurring. Another is that the scheme can automatically stop smoothing at some optimal points, and the continued application of this scheme produces no further change. The key idea in the Max/Min flow scheme is to introduce a Max/Min switch function into the decision of the local optimal motion for noise removal. In this section, we generalize this framework, and try to suppress boundary leaking under this general framework on image segmentation and region tracking applications in the following section.

We refer to a speed function F in the context of the general level set equation $\phi_t = F|\nabla\phi|$, where F is assigned the speed of the front in a direction opposite to its normal direction. The generalized Max/Min flow framework can be written as,

$$F(X) = \begin{cases} \min(F_c(X), 0), & \text{satisfying decision rules} \\ \max(F_c(X), 0), & \text{otherwise} \end{cases}, \quad (3)$$

where the decision rules can be designed specially for various applications. Actually, it lies on F_c but not this generalized framework whether the level set equation has a trivial steady state solution.

First, we consider the following two flows, $F = \min(F_c, 0)$ and $F = \max(F_c, 0)$. When the level set function ϕ is chosen the negative of the signed distance in the interior, and the positive sign in the exterior region, the flow under $F = \min(F_c, 0)$ will tend to grow outward endlessly. Conversely, the flow under $F = \max(F_c, 0)$ will tend to shrink until collapse to a point. Very roughly speaking, we might think of the choice of the Max and Min flow related to the evolving tendency, i.e. the evolving tendency of the flow under Eq.(3) depends on the choice of the max and min flows, while the evolving tendency of the flow under $F = F_c$ only depends on F_c .

Then, let the flow under $F = F_c$ corresponding to the level set equation $\phi_t = F_c|\nabla\phi|$ be able to reach a trivial steady state solution. Note that the steady state solution is only a local optimal solution of the above equation, and it is not unique. And the choice of flow under Eq.(3) is either F_c or zero.

After that, we consider the flow F_c under this generalized framework again. If the choice of flow resulted from the decision rules in Eq.(3) and the flow

under $F = F_c$ are identical at all the time, it is clear that a steady state solution of Eq.(3) is namely one of the flow under $F = F_c$. On the other hand, the worse case occurs when the choice resulted from the decision rules in Eq.(3) and the flow under $F = F_c$ have opposite evolving tendency, i.e. the speed is always set to zero, $F = 0$. No propagation takes place in this case. In addition, if the Max/Min flow stays at some state that is a steady state for the flow under $F = F_c$, it is clear that $F_c = 0$ in this case. Then, whether the Max or Min flow is selected in Eq.(3), no propagation takes place.

When they have the same evolving tendency on some local parts of the evolving curve, these parts will tend to a steady state just as they are driven by the flow under $F = F_c$. When the opposite evolving tendency appears on other parts of the evolving curve, then no propagation takes place. Hence, if only the choice of flow under Eq.(3) and the flow under $F = F_c$ are identical, the propagation takes place, just as the front of propagation is driven by the flow under $F = F_c$. The final steady state solution of the scheme of Eq.(3) should be bounded by all steady state solutions which the flow under $F = F_c$ can reach. From above analysis, we yield

Proposition: If the flow under $F = F_c$ can reach a steady state, this flow under the generalized Max/Min flow framework is able to reach a steady state too.

In addition, this general framework is an open general computational framework, under which many constraint conditions can be coupled in the speed function to suppress boundary leaking. We illustrate it on the image segmentation and region tracking applications in the following sections. It can be noticed that they would have the same form of F_c in their speed functions, except their different decision rules.

4. Applications

4.1 Image Segmentation Under Generalized Max/Min Flow Framework

Under the generalized Max/Min flow framework, the geodesic active contour model is still adopted, while the decision rules are concerned in this section. Our proposed algorithm is to aim at the partial volume estimation, which is a boundary leaking problem essentially. Usually, this kind of problems indicates that the risk of misclassification for adjacent regions is too big, and in some extreme cases where the two distributions have the same mean but different variances, the classification error will be intolerable. In order to overcome these problems, some further texture features are extracted as the vector

feature. In this paper, for the analysis convenience, we consider Gaussian distributions, and the number of classes is supposed known so as to estimate the parameters of statistic model.

In order to deal with the finite mixture model, we choose some clique types shown in Fig.1 and intensity feature as the pixel feature vector. These clique types as texture features have been applied into the texture image segmentations [16]. The feature vector $\mathbf{V}(X) = (v_1(X), \dots, v_m(X), v_{m+1}(X))^T$, $X \in R^2$ is defined

$$\text{by } \begin{cases} v_i(X) = \sum_{c \in C_i} \Delta_c(X), & i \leq m \\ v_{m+1}(X) = \frac{1}{w \times w} \sum_{X \in W} I(X), & i = m+1 \end{cases}, \text{ where, } C_i$$

is the set of all cliques of type i in a given window $W(w \times w)$, $\Delta_c(X) = -1$ if $I(X) = I(X')$ and $\Delta_c(X) = 1$ otherwise. In our algorithm, the feature number $m+1 = 5$. It is easy to see that the first m elements are texture features while the $(m+1)$ th is the intensity feature. So, these features should allow to be applied in both textured and non-textured images.

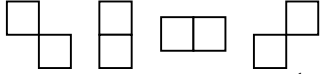


Fig.1 The 4 clique types associated to a 2nd order model

Suppose that the feature vectors satisfy the Gaussian distribution, i.e. $\mathbf{V}(X) \sim \mathcal{N}(\mathbf{m}, \Sigma)$. After these feature vectors are extracted, the EM algorithm is applied to estimate the parameters for each class in image. Since the elements in $\mathbf{V}(X)$ are not independent each other, the probability density function $pd_i(\mathbf{V}(X))$ should be a higher dimension Gaussian form for each class $R_i, R = \bigcup_i R_i$. In order to estimate the probability of each pixel robustly, we can sample a neighbor window around the each pixel. For the partial mixture case in a given window, the above probability density function will be replaced by the joint probability density function for each class,

$$\log pd_i(\mathbf{V}(X) | \mathbf{m}_i, \Sigma_i) = \sum_{Y \in W(X)} \alpha_i \log pd_i(\mathbf{V}(Y) | \mathbf{m}_i, \Sigma_i)$$

where, $\alpha_i = \|R_i \cap W\| / (w \times w)$, which made the mixture distribution of X , $\Pr(\mathbf{V}(X)) = \prod_i pd_i(\mathbf{V}(X) | \mathbf{m}_i, \Sigma_i)$, depend on the position $X(x, y) \in R^2$. Because of $\mathbf{V}(X) \sim \mathcal{N}(\mathbf{m}, \Sigma)$ for a given window $W(X)$, its sample mean $\bar{\mathbf{V}}(X)$ and covariance matrix $\bar{\Sigma}(X)$ should satisfy the Gaussian distribution too. In [12], the above joint probability density function for each class was rewritten as,

$$\log pd_i(\mathbf{V}(X) | \mathbf{m}_i, \Sigma_i) = -\frac{1}{2} \left[(\bar{\mathbf{V}}(X) - \mathbf{m}_i)^T \Sigma_i^{-1} (\bar{\mathbf{V}}(X) - \mathbf{m}_i) + \text{tr}(\Sigma_i^{-1} \bar{\Sigma}(X)) + \log(2\pi \det(\Sigma_i)) \right]$$

It is clear that the above equation can detect two regions with the same means but different variances.

At last, a Bayesian classification method is applied to decide which class each pixel should belong to by the following likelihood function,

$$\Pr(X | \mathbf{m}_i, \Sigma_i) = \frac{\Pr(\mathbf{m}_i, \Sigma_i) \cdot pd_i(\mathbf{V}(X) | \mathbf{m}_i, \Sigma_i)}{\sum_i \Pr(\mathbf{m}_i, \Sigma_i) \cdot pd_i(\mathbf{V}(X) | \mathbf{m}_i, \Sigma_i)},$$

where the prior probability $\Pr(\mathbf{m}_i, \Sigma_i)$ can be estimated by EM algorithm. The Bayesian classification result is the class number,

$$L(X) = \arg \max_i (\Pr(X | \mathbf{m}_i, \Sigma_i))$$

Because the inside of evolving curve is viewed as a single region R_{L_0} , the decision rules only need to decide whether the Bayesian classification result $L(X)$ is equal to the class number L_0 . Under the Max/Min flow framework, the curve evolution equation for segmentation can be rewritten as,

$$\phi_t = F |\nabla \phi| \quad (4)$$

$$\text{where, } F = \begin{cases} \min\{(g(|\nabla I|) \kappa_c - \nabla g \cdot \mathbf{N}_c), 0\}, & L(X) = L_0 \\ \max\{(g(|\nabla I|) \kappa_c - \nabla g \cdot \mathbf{N}_c), 0\}, & \text{otherwise} \end{cases}$$

Compared with the scheme of Eq.(1), the scheme of Eq.(4) increases capture range, and selects a reasonable evolution direction for each iteration step. Since the Bayesian decision can control the evolution tendency of the evolving curve under the generalized Max/Min flow framework.

4.2 Region Tracking Under Generalized Max/Min Flow Framework

As the image segmentation, we mostly concern about the decision rules under this generalized framework. The scheme of Eq.(2) consists of the two parts, one is the motion detection, and another is the tracking part. First, consider the equation of the motion detection. The crucial step is to decide whether the current pixel belongs to the moving area. Since the inter-frame difference probability density function is modeled as a mixture of two Gaussian (or Laplacian) distributions. It can be written as,

$$pd(d(X)) = P|_{bg} \cdot pd|_{bg}(d(X)) + P|_{obj} \cdot pd|_{obj}(d(X))$$

where, $P|_{bg} (, P|_{obj})$ is a priori probability under the background (, object) area case. We can design the decision rule for the equation of motion detection according to the above equation. Under the generalized Max/Min flow framework, the equation of motion detection can be re-written as,

$$\phi_t = F_D |\nabla \phi|,$$

where,

$$\begin{cases} F_D = \min \left(g(I_D)\kappa_c + \nabla g(I_D) \cdot \frac{\nabla \phi}{|\nabla \phi|}, 0 \right), \\ \quad P|_{bg} \cdot pd|_{bg}(d(X)) < P|_{obj} \cdot pd|_{obj}(d(X)) \\ F_D = \max \left(g(I_D)\kappa_c + \nabla g(I_D) \cdot \frac{\nabla \phi}{|\nabla \phi|}, 0 \right), \\ \quad \text{otherwise} \end{cases}$$

The motion detection is similar to the image segmentation, only its input frame is the enhancement frame $\{I_D\}$. In order to increase the capture range, we can apply the above image segmentation approach into frame $\{I_D\}$. Since there are only the object area and background area in frame $\{I_D\}$, the class number is two. And the feature is the scale $d(X)$, which is simplified as $d(X) \sim \mathcal{N}(0, \sigma^2)$. Similarly to the image segmentation case, we sample a neighbor window around the point X . The joint probability density function for each class can be rewritten as,

$$\log pd_i(d(X)|\sigma_i^2) = -\frac{1}{2} \left[\log(2\pi\sigma_i^2) + \frac{\bar{d}^2(X)}{\sigma_i^2} + \frac{\bar{\sigma}^2(X)}{\sigma_i^2} \right], i=1,2$$

where, $\bar{d}(X)$ and $\bar{\sigma}^2(X)$ are the window mean and variance respectively. We can easily yield the Bayesian decision by the following likelihood function,

$$\Pr(X|\sigma_i^2) = \frac{\Pr(\sigma_i^2) \cdot pd_i(d(X)|\sigma_i^2)}{\sum_i \Pr(\sigma_i^2) \cdot pd_i(d(X)|\sigma_i^2)}, i=1,2.$$

So, the speed function can be re-defined as,

$$\begin{cases} F_D = \min \left(g(I_D)\kappa_c + \nabla g(I_D) \cdot \frac{\nabla \phi}{|\nabla \phi|}, 0 \right), \\ \quad \Pr(X|\sigma_{bg}^2) < \Pr(X|\sigma_{obj}^2) \\ F_D = \max \left(g(I_D)\kappa_c + \nabla g(I_D) \cdot \frac{\nabla \phi}{|\nabla \phi|}, 0 \right), \\ \quad \text{otherwise} \end{cases} \quad (5)$$

For the equation of tracking part, the crucial step is to decide the evolving direction of evolution curve (i.e. the direction of the object motion). Because the edges or a texture background in the original input frame could often change the evolving direction unpredictably. In [15], the probability of each pixel belonging to the inside and outside of evolving curve can be approximated by the infimum of the inter-frame intensity difference. Obviously, the estimate of infimum can be used in the decision rules for the equation of tracking part under the generalized Max/Min flow framework. The equation of tracking part can be re-written as,

$$\phi_t = F_T |\nabla \phi|$$

where,

$$\begin{cases} F_T = \min \left(g(|\nabla I|)\kappa_c + \nabla g(|\nabla I|) \cdot \frac{\nabla \phi}{|\nabla \phi|}, 0 \right), V_{in} < V_{out} \\ F_T = \max \left(g(|\nabla I|)\kappa_c + \nabla g(|\nabla I|) \cdot \frac{\nabla \phi}{|\nabla \phi|}, 0 \right), \text{ otherwise} \end{cases}, (6)$$

$$\begin{cases} V_{in} = \inf_{\{Z|Z|\leq\delta, X+Z\in\Omega\}} (I(X,t) - I(X+Z,t-1))^2 \\ V_{out} = \inf_{\{Z|Z|\leq\delta, X+Z\in\bar{\Omega}\}} (I(X,t) - I(X+Z,t-1))^2 \end{cases}$$

The parameter δ determines the maximum range of motion. So, it should be set to different values for the different image sequences respectively.

According to Eq.(5) and Eq.(6), the scheme of (2) is redefined as,

$$\phi_t = (F_D + F_T) \cdot |\nabla \phi|. \quad (7)$$

Although the motion detection and tracking part have the same form of speed function as in image segmentation, they are two different problems, which can be solved by their different decision rules. Thus, the speed function becomes simple and flexible. In fact, the Max/Min flow framework is only a general computational framework. Under this framework, we can only consider the intrinsic characteristics to design speed function, while leave the ‘‘stop criterion’’ in decision rule. In this way, many methods and strategies can be introduced into the decision rules.

4.3 Experiments

Image Segmentation

The experiment of image segmentation is leg bone segmentation on a gray slice image. From the original slice image in Fig.(2a), it can be observed that the boundary of bone is blurry, but the texture features between the different regions are distinct. So, the texture features are used in our algorithm. In this experiment, our algorithm is used to deal with the partial volume estimation. An initial segmentation should be given. We can usually obtain it using K-means method (see Fig.(2b)). The image segmentation is implemented by the schemes of Eq.(1) and Eq.(4) respectively. The function $g(f)$ in the evolution equations is defined as $g(f) = 1/(1+|f|^k)$, $k=1$ or 2 .

The segmented image by Eq.(1) is shown in Fig.(2c). Since some parts of the evolving curve in the initial segmented image have run across the edges of leg bone while others have not reached the boundary, the evolving curve by Eq.(1) only reached some local edges of texture but not the desired boundary of leg bone when a steady state was reached. It is distinct that the flow under Eq.(1) leaks through the boundary on some locations of the desired boundary after continued application of scheme of

Eq.(1). When the image segmentation is driven by Eq.(4), the evolving curve can trend towards the boundaries of leg bone gradually, and converge to them finally. The segmented image by Eq.(4) is shown in Fig.(2d).

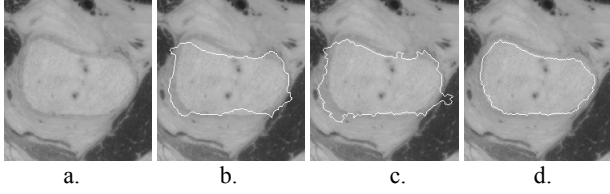


Fig.2 Image segmentation by the schemes of (1) and (4)

Region Tracking

The experiments of region tracking are carried out on 320×240 resolution grey image sequence. The two methods driven by the schemes of (2) and (7) are compared from the following three aspects, motion detection part, tracking part and combined equation.

Motion Detection

We detect the moving area by the implementations of the motion detection part in Eq.(2) and in Eq.(7) respectively. In this experiment, the Gaussian model is adopted. Some unknown parameters can be estimated by EM algorithm for creating the enhancement frame $\{I_D\}$ and defining decision rules.

The enhancement frame $\{I_D\}$ is shown in Fig.(3b). It can be seen that the moving area has been enhanced from background. We perform the motion detections in the schemes of (2) and (7) on the new frame $\{I_D\}$ respectively until a steady state is reached. The results are shown in Fig.(3c,3d). It can be noticed that the evolving curve by the motion detection in Eq.(2) is prone to getting across the boundaries with a small gradient magnitude.

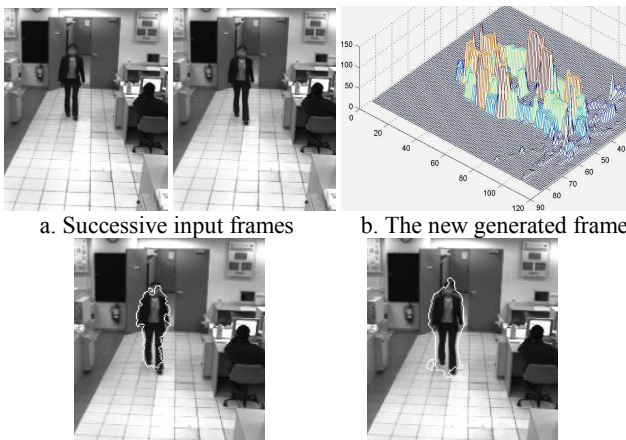


Fig.3 Motion detection

Tracking Part

The contour of the moving object is tracked by the implementations of the tracking part in Eq.(2) and in Eq.(7) respectively. The former is only based on the current frame $\{I_n\}$, but the latter is based on both the current frame $\{I_n\}$ and previous frame $\{I_{n-1}\}$. The evolving curves in Fig.(3c,3d) are defined as the initial zero level sets for tracking part. The evolution results are shown in Fig.(4). It can be noticed that the evolving curve by the scheme of (6) can converge to the boundary of the moving object.



Fig.4 The comparison of the tracking parts

Combined Equation

In this experiment, we illustrate our tracking algorithm via the implementation of the scheme of Eq.(7) on a real image sequence under the generalized Max/Min flow framework. For the computational conveniences, the initial contour is manually outlined in the first frame 0 of the sequences, and then the contour is tracked from the frame 0 to frame 1, then from frame 1 to frame 2, and so on until the last frame in the sequence. The total of frames is 30. The initial unknown parameters in Gaussian models can be estimated accurately using the contour area in the first frame, and then these parameters could be estimated repeatedly using the known contour area in previous frame. The results are shown in Fig.(5).

In the first 19 frames, the inter-frame motion is little. The motion detection part in Eq.(7) can easily locate the motion area, which is very close to the boundaries of moving object. So, the tracking part in Eq.(7) can refine the evolving curve to converge at the contour of the moving object in a small range. The parameter δ can be set a little value.

After frame 20, the moving object is becoming fast at the image speed of about 10 pixels per frame. Although the motion detection part in Eq.(7) could detect the motion area, the area is very large to the boundaries of moving object. A lot of edges or texture on the background appear in this motion area. Hence, the motion detection part is not available for detecting the boundaries of object. It is difficult to tracking the boundaries of object by the tracking part in Eq.(7) in this complicated area. In frame 20, it can be noticed that the evolving curve converges at the boundaries of other object but not moving object. Although we tried to adjust some

parameters, such as δ is set a large value, the obtained contour of the moving object is apparently deformed.

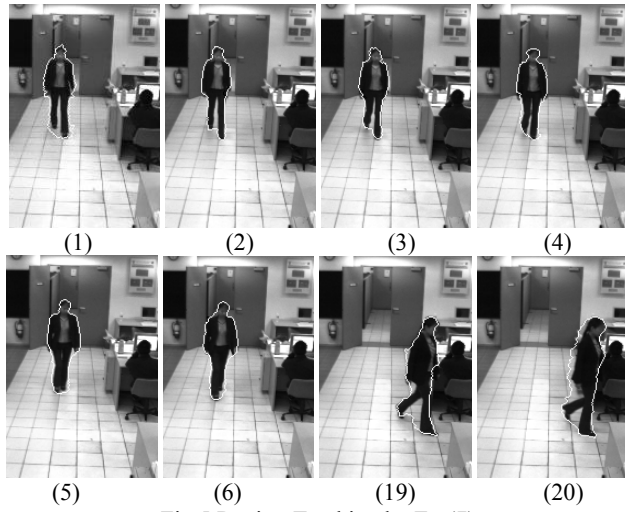


Fig.5 Region Tracking by Eq.(7)

5. Conclusions

In this paper, we firstly analyzed how to result in boundary leaking on the geodesic active contour model in detail. Then, the Max/Min flow framework was generalized as a general computational framework, and applied to deal with boundary leaking on the image segmentation and region tracking applications. It was proved that the generalized Max/Min flow framework could reach a steady state solution. From the above applications, it can be noticed that many methods and strategies could be introduced into this generalized framework as the decision rules, so as to suppress boundary leaking. From an implementation point of view, the speed function becomes simple and flexible under this general framework.

In future work, we will develop more robust methods or techniques as the decision rules under the generalized Max/Min flow framework, so as to overcome boundary leaking, but not only suppress it.

References

- [1] M. Kass, A. Witkin, and D. Terzopoulos, Snakes: Active Contour Models, *Int'l J. Computer Vision*, Vol.1, pp.321-332, 1988
- [2] V. Caselles, R. Kimmel, and G. Sapiro, Geodesic Active Contours, *Int'l J. Computer Vision*, Vol.22, pp.61-79, 1997
- [3] S. Osher and J. Sethian, Fronts Propagating with Curvature-Dependent Speed: Algorithms Based on the Hamilton-Jacobi Formulation, *J. Computational Physics*, Vol.79, pp.12-49, 1988
- [4] J. Gomes and O. Faugeras, Level Sets and Distance Functions, in *Proc. of 6th European Conference on Computer Vision*, Dublin, Ireland, Vol.1, pp.588-602, 2000
- [5] K. Siddiqi, Y. Lauziere, and A. Tannenbaum, et al., Area and Length Minimizing Flows for Shape Segmentation, *IEEE Trans. On Image Processing*, Vol.7, No.3, pp.433-443, 1998
- [6] N. Paragios, O. Mellina-Gottardo and V. Ramesh, Gradient vector flow fast geodesic active contours, in *Proceedings of IEEE Int'l Conf. On Computer Vision*, Vol.1, pp.67-73, Vancouver, Canada, 2001
- [7] B. Sumengen, B.S. Manjunath, and C. Kenney, Image segmentation using curve evolution and flow fields, *IEEE Int'l Conf. On Image Processing*, Vol.1, pp.105-108, Rochester, NY, USA, 2002
- [8] R. Malladi and J. Sethian, *Image Processing: Flows under Min/Max Curvature and Mean Curvature*, Graphical Models and Image Processing, Vol.58, No.2, pp.127-141, 1996
- [9] R. Malladi and J. Sethian, A Unified Approach to Noise Removal, Image Enhancement, and Shape Recovery, *IEEE Trans. on Image Processing*, Vol.5, No.11, pp.1554-1568, 1996
- [10] D.H. Laidlaw, K.W. Fleischer and A.H. Barr, Partial-Volume Bayesian Classification of Material Mixtures in MR Volume Data Using Voxel Histograms, *IEEE Trans. on Medical Imaging*, Vol.17, No.1, pp.74-86, 1998
- [11] D. Williamson, N. Thacker, et al., Partial Volume Tissue Segmentation using Grey-Level Gradient, in *Proc. of Medical Image Understanding and Analysis*, Portsmouth, UK, 2002
- [12] S.C. Zhu and A. Yuille, Region Competition: Unifying Snakes, Region Growing, and Bayes/MDL for Multiband Image Segmentation, *IEEE Trans. on Pattern Analysis and Machine Intelligence*, Vol.18, No.9, pp.884-900, 1996
- [13] N. Paragios and R. Deriche, Geodesic Active Contours and Level Sets for the Detection and Tracking of Moving Objects, *IEEE Trans. on Pattern Analysis and Machine Intelligence*, Vol.22, pp.266-280, 2000
- [14] N. Paragios and G. Tziritis, Detection and Location of Moving Objects Using Deterministic Relaxation Algorithms, in *Proc. of IAPR International Conference on Pattern Recognition*, pp.201-205, Aug. 1996, Vienna, Austria
- [15] A. Mansouri, Region Tracking via Level Set PDE's without Motion Computation, *IEEE Trans. on Pattern Analysis and Machine Intelligence*, Vol.24, pp.947-961, 2002
- [16] M. Roula, A. Bouridane, and A. Amira, et al., A Novel Technique for Unsupervised Texture Segmentation, in *Proc. of IEEE Int'l Conf. on Image Processing*, Vol.1, pp.58-61, Thessaloniki, Greece, 2001